

Femtosecond control of phonon dynamics near a magnetic order critical point

Oleg Gorobtsov (✉ gorobtsov@cornell.edu)

Cornell University

Louis Ponet

Italian Institute of Technology

Sheena Patel

Department of Physics, University of California San Diego

Nelson Hua

University of California, San Diego

Anatoly Shabalin

University of California, San Diego

Stjepan Hrkac

University of California, San Diego

James Wingert

University of California-San Diego

Devin Cela

University of California, San Diego

James Glowia

SLAC National Accelerator Laboratory

Diling Zhu

SLAC National Accelerator Laboratory

Rajasekhar Medapalli

National Institute of Technology Andhra Pradesh

Matthieu Chollet

Linac Coherent Light Source, SLAC National Accelerator Laboratory

E.E. Fullerton

Center for Magnetic Recording Research, University of California San Diego, La Jolla, CA 92093-0401, USA. <https://orcid.org/0000-0002-4725-9509>

Sergey Artyukhin (✉ Sergey.Artyukhin@iit.it)

Italian Institute of Technology

Oleg Shpyrko

University of California, San Diego

Andrej Singer (✉ asinger@cornell.edu)


University of California, San Diego

Article

Keywords: spin-phonon interaction, spin density wave, photoexcitation, X-ray Free-Electron Laser, vibrational state, Landau theory

Posted Date: July 21st, 2020

DOI: <https://doi.org/10.21203/rs.3.rs-40430/v1>

License:  This work is licensed under a Creative Commons Attribution 4.0 International License.
[Read Full License](#)

Version of Record: A version of this preprint was published at Nature Communications on May 17th, 2021. See the published version at <https://doi.org/10.1038/s41467-021-23059-2>.

Femtosecond control of phonon dynamics near a magnetic order critical point

O. Yu. Gorobtsov^{1†}, L. Ponet^{2,3†}, S. K. K. Patel^{4,5}, N. Hua^{4,5}, A. G. Shabalin⁴, S. Hrkac⁴, J. Wingert⁴, D. Cela⁴, J. M. Glowina⁶, D. Zhu⁶, R. Medapalli^{5,7}, M. Chollet⁶, E. E. Fullerton⁵, S. Artyukhin^{2*}, O. G. Shpyrko^{4,5}, A. Singer^{1*}

1 – Materials Science and Engineering Department, Cornell University, Ithaca, NY 14853, USA

2 – Central Research Labs, Italian Institute of Technology, Genova, Italy

3 - Scuola Normale Superiore, Pisa, Italy

4 – Department of Physics, University of California, San Diego, La Jolla, California, 92093, USA

5 - Center for Memory and Recording Research, University of California, San Diego, La Jolla, California, 92093, USA

6 - The Linac Coherent Light Source, SLAC National Accelerator Laboratory, Menlo Park, CA 94025 USA

7 - Department of Physics, School of Sciences, National Institute of Technology, Andhra Pradesh 534102, India

*Correspondence to: asinger@cornell.edu, sergey.artyukhin@iit.it

† - These authors contributed equally to this work

The spin-phonon interaction in spin density wave (SDW) systems often determines the free energy landscape that drives the evolution of the system [1] [2]. When a passing energy flux, such as photoexcitation [3], drives a crystalline system far from equilibrium [4] [5], the resulting lattice displacement generates transient vibrational states. Manipulating intermediate vibrational states in the vicinity of the critical point, where the SDW order parameter changes dramatically, would then allow dynamical control over functional properties. Here we combine double photoexcitation [6] with an X-ray Free-Electron Laser (XFEL) probe [7] [8] to control and detect the lifetime and magnitude of the intermediate vibrational state near the critical point of the SDW. We apply Landau theory to identify the mechanism of control as a repeated partial quench and sub picosecond recovery of the SDW. Our results showcase the capabilities to influence and monitor quantum states by combining multiple optical photoexcitations with an XFEL probe. They open new avenues for manipulating and researching the behaviour of photoexcited states in charge and spin order systems near the critical point.

If an energy flux passing through the system induces a phase transition far from thermal equilibrium, the pathway of the transition changes significantly, and intermediate states can arise in the material [2] [3]. In particular, inhomogeneous excitations produce a lattice displacement in crystalline materials, generating intermediate vibrational states. In materials with a SDW state, vibrational states interact with spin order [5], leading to effects such as a re-emergence of a suppressed SDW [9]. On the other hand, suppressing the intermediate states allows reproducing adiabatic transitions on much faster timescales - an approach termed "shortcuts to adiabaticity" (STA) in quantum technology [10] [11] [12]. Manipulation of photoexcited density wave

states also has possible applications in fast switching devices [13, 14]. Therefore, generating a designed vibrational state in spin systems by enhancing or suppressing spin-phonon interactions opens ways to precise manipulation of spin and lattice systems.

A promising path for altering intermediate states and the energy landscape is to leverage the critical behaviour near a phase transition, where the degree of order in the system changes rapidly with temperature. Elemental chromium serves as an ideal material for studying critical behaviour: an incommensurate SDW [5] in chromium gives rise to a second-harmonic periodic lattice distortion (PLD) and a charge density wave (CDW) at relatively high temperatures (308 K in bulk, 290 K in the 30-nm film studied here), rendering the critical behaviour close to the SDW phase transition highly accessible. Thin antiferromagnetic films with SDW states are especially important for devices utilizing spin transport [15] [16], and sustain a unidirectional SDW and discrete SDW periods due to pinning at the interfaces [17] [18]. The magnetostrictive coupling between SDW and PLD allows for the excitation of acoustic phonons by fully or partially quenching the SDW order parameter throughout the film with a photoexcitation [8] [19, 20]. Previous studies have shown that when the energy flux at the film is at or below ~ 2 mJ/cm², the spin order recovers before the acoustic phonon decays [8], transiently enhancing the PLD above its value in equilibrium [5]. The ultrafast recovery of the SDW should enable a repeated quench that acts as a lever to further enhance or suppress the oscillation of the PLD.

High precision measurements of the PLD are necessary to detect and control the changes in the spin and lattice structure effectively. XFELs offer time resolution down to femtoseconds in pump-probe experiments, making them a powerful tool to study PLD dynamics [7]. X-ray scattering intensity in a satellite PLD peak is directly proportional to the magnitude of the PLD [21, 5, 22], enabling a quantitative measurement of both amplitude and phase of the lattice oscillation. X-ray measurements offer an advantage over recently matured ultrafast electron diffraction [23, 24]: the Bragg angles are generally large and the peaks are narrow, which provides higher peak selectivity and enables measurements of thin films grown epitaxially on a thick crystalline substrate. Moreover, X-rays directly couple to the core electrons, overcoming the challenges of the optical pump-probe methods [6, 25, 13] where screening effects make an interpretation challenging. In addition, unlike optical reflectivity, X-ray measurements are not hindered by the surface roughness of the film.

Here, we use two consecutive laser pulses [12, 25, 6] to drive the system out of equilibrium; the separation between the pulse arrival times τ_1 and τ_2 modifies the response of the system (see for ex. [6]). The first 40 fs laser pulse quenches the electronic and spin order throughout the entire 28 nm Cr film (see Methods for details), releasing an acoustic phonon with wavevector normal to the surface and an oscillation period of approximately 450 fs. In less than a picosecond, the electronic subsystem thermalizes with the lattice below the Néel temperature, and the SDW and CDW orders recover [26] [8] [27]. The acoustic phonon has a damping time of about 3 ps [8]. If a second laser pulse arrives before the excited state diminishes, it is possible to either further excite, sustain, or completely dampen the excited state (Fig. 1 (a)). Further evolution of the system depends on the phase and amplitude of the phonon in that moment. An X-ray probe pulse of 50-fs duration scatters on the atomic structure of the film at a delay time t , and the PLD in the crystal gives rise to a satellite peak on the Laue fringes of the out-of-plane (002) crystal Bragg peak (Fig. 1 (a), inset). An XFEL pulse 0.2 mm in diameter envelopes

multiple SDW domains [28] below the Néel temperature, making the measurement statistical over domains.

Evolution of the PLD as a function of the probe delay t presented in Figs. 1 (b, c) for 2 different $\tau_2 - \tau_1$ shows that we are indeed able to completely suppress or further enhance the excited state with the second pulse. The magnitude of the PLD oscillation - excited acoustic phonon - reaches 125% of the unperturbed lattice distortion. The absolute value of the PLD after both photoexcitations reaches 150%. The variation in PLD is thus 6 times larger than the total relative drop of 20% in the PLD after 9 ps when the film equilibrates at a new film temperature. An excitation of such a magnitude is distinctly different from the conventional displacive excitation mechanism, where the ratio is about one [8] [29] (See Fig. 2 c).

Figure 2 (a) demonstrates how the amplitude of the PLD changes with both $\tau_2 - \tau_1$ and the probe delay t . The frequency of the acoustic phonon remains unchanged, but its amplitude changes periodically with the pump-pump delay. After 9 ps from the last excitation, the PLD stabilizes at a delay-independent level: the lattice and electrons are in the thermal equilibrium and the subsequent heat transport to the substrate occurs over ~ 1 ns timescale [21]. When $|\tau_2 - \tau_1|$ is shorter than the time of the SDW recovery, we observe an approximately 2 times weaker excited phonon (Fig. 2 (a)), as the second pulse merely increases the overall temperature of the system without displacive excitation [29]. The effect remains even if the second pulse is weakened by a factor of 2 (Fig. 2 (b)), leaving the short-term electron temperature below T_N . At the first pulse fluence $P_1 > 3 \text{ mJ/cm}^2$, the overall temperature of the system rises above T_N , and the system is indifferent to the second pulse arrival time τ_2 : compare Fig. 2 (c) top and bottom. The magnetic order is destroyed after the first pulse and does not recover; therefore, the second pulse has a negligible effect on the phonon dynamics. Interestingly, we do not observe a prolonged order recovery on the scale of several picoseconds associated with the removal of topological defects [3] (see Methods).

In order to better interpret the experimental data, we put forward a phenomenological model in the spirit of Landau theory [30] with order parameters L and Ψ describing the amplitudes of the SDW and the PLD, related to the Fourier component of the spin density at the SDW wave vector q , $L = S_q$ and to the related acoustic phonon amplitude $\Psi = u_{2q}$, respectively (Fig. 3a). The essential energetics of the interacting PLD and SDW can be captured by the Landau free energy,

$$F = \frac{\alpha}{2} (T_{SDW} - T_N) L^2 + \frac{\beta}{4} L^4 - g L^2 \Psi + \frac{m \omega_0^2}{2} \Psi^2 + \frac{\gamma}{4} \Psi^4, \quad (1)$$

where T_{SDW} is the system temperature, T_N is the Néel temperature; the terms with α and β describe the double-well potential acting on the SDW amplitude L . The lowest-order interaction term between SDW and PLD, with the coupling constant g , couples the PLD amplitude to the square of the time reversal-odd SDW order parameter, for the energy to be time reversal-even. Parameters m, ω_0, γ are the mass, the frequency, and the anharmonicity of the acoustic phonon. In order to describe the heat injection and transfer between spin and phonon reservoirs, we supplement Eq. (1) with a two-temperature model (see Methods) to compute the PLD dynamics (see methods). As the SDW is heated by pump pulses and subsequently cooled by the heat transfer to the phonon bath, the interaction between SDW and PLD exerts a force on PLD, that drives PLD oscillations.

Below T_N , the non-zero PLD is induced by the SDW order L . Close to T_N , PLD magnitude depends on $L \sim \sqrt{T_{SDW} - T_N}$ within the mean-field approximation. When the laser pulse quenches the SDW, L rapidly decreases and then returns to its equilibrium value within ~ 0.5 ps as the system cools. Through the coupling constant g , these changes of L launch an oscillation in Ψ . The SDW amplitude L saturates at temperatures well below the Néel temperature ($T \ll T_N$) but is strongly sensitive to T near the phase transition. Therefore, the oscillation is induced most effectively in the temperature range close to the critical point. On the other hand, exceeding the critical temperature suppresses the spin order, so the force exerted on Ψ does not increase further, leading to a diminished momentum transfer to Ψ . Since the force induced via g -coupling is proportional to $L^2 = \alpha^2(T_N - T)$ when $T < T_N$ and zero otherwise, to maximize the momentum of Ψ achieved after the first pulse we must tune the intensity of the first pulse to melt the SDW order but not heat the system further. Therefore, until the SDW order is restored at least partially, no further momentum can be transferred, leading to the horizontal stripe with a relatively low oscillation amplitude around zero pump-pump delay ($T_1 = T_2$) when both pump pulses come almost simultaneously (Fig. 3 (d), cf. experimental Fig. 2 (a,b)). If the SDW order is partially melted, and the second pulse hits after it is restored, Ψ gains extra momentum. Depending on the phase of the second pulse with respect to the first one, this extra momentum can be along or opposite to that already present, therefore increasing or decreasing the oscillation amplitude, as seen from experiments in Figs. 1 and 2. This is exactly why multiple pulses, spaced at optimal delays, are essential to maximize the phonon amplitude. Our theoretical model provides an excellent quantitative agreement with the experiment, as Figs. 3 (d, e) demonstrates.

The excellent agreement between theory and data allows us to speculate on the broader control possibilities based on the theoretical parameters extracted from our experiments. By further splitting the laser pulse into a longer pulse train, a further control over a sustained excited state would be possible (Fig. 4). Simulations performed for Figs. 4 (b, c) using our experimental model demonstrate a possibility to generate complicated intermediate vibrational states, for example with sawtooth (Fig. 4 (b)) and sinusoidal (Fig. 4 (c)) oscillation envelopes. The material would then be suspended in dynamic equilibrium with the pulse train configuration as a control parameter. In the studied system, the intensity of an individual pulse in such a train must be kept below approximately 0.1 mJ/cm^2 so that the total deposited heat dissipates into the substrate and the equilibrium temperature does not rise above T_N .

This work establishes an FEL X-ray probe combined with multiple optical photoexcitations in the vicinity of a critical point as a promising path to robust ultrafast control of photoexcited states. The ultrafast X-ray probe serves as a high precision feedback to the optical double pump setup, enhancing our understanding of underlying processes and therefore possibilities for control. The precision of PLD measurements let us develop a quantitative model as a guide to future developments. Our results pave a way to ultrafast driving of complex spin and charge ordered systems, revealing details of electron-phonon and spin-phonon coupling, especially near criticality.

Acknowledgements

The work was supported by U.S. Department of Energy, Office of Science, Office of Basic Energy Sciences, under Contracts No. DE-SC0019414 (ultrafast x-ray data

analysis and interpretation O.G., A. Si), DE-SC0001805 (ultrafast x-ray scattering experiments, A.S.) and No. DE-SC0018237 (thin films synthesis and characterization, ultrafast x-ray scattering, S. K. K. P., and E.E.F.). Use of the Linac Coherent Light Source (LCLS), SLAC National Accelerator Laboratory, is supported by the U.S. Department of Energy, Office of Science, Office of Basic Energy Sciences under Contract No. DE-AC02-76SF00515.

Author contribution

A. Si, O. G. S. and E. E. F. planned the project; A. Si., S. K. K. P., A. Sh., N. H., S. H., R. M., J. W., D. C., J. M.G, D. Z., M. C. performed the pump-probe x-ray measurements; O. G. performed data analysis and interpretation of the results; L. P. and S. A. worked on the theory; S. K. K. P. and E. E. F. grew samples; and O. G., L. P., S. A., and A. Si. wrote the paper. All authors contributed to discussions and gave comments on the manuscript.

Competing Interests statement

The authors declare no competing interests.

Bibliography

- [1] K. Nasu, Photoinduced Phase Transitions, World Scientific, 2004.
- [2] H. Haken, "Cooperative phenomena in systems far from thermal equilibrium and in nonphysical systems," *Reviews of Modern Physics*, vol. 47, pp. 67-121, 1 1975.
- [3] A. Zong, A. Kogar, Y.-Q. Bie, T. Rohwer, C. Lee, E. Baldini, E. Ergeçen, M. B. Yilmaz, B. Freelon, E. J. Sie, H. Zhou, J. Straquadine, P. Walmsley, P. E. Dolgirev, A. V. Rozhkov, I. R. Fisher, P. Jarillo-Herrero, B. V. Fine and N. Gedik, "Evidence for topological defects in a photoinduced phase transition," *Nature Physics*, vol. 15, pp. 27-31, 10 2018.
- [4] D. N. Basov, R. D. Averitt and D. Hsieh, "Towards properties on demand in quantum materials," *Nature Materials*, vol. 16, pp. 1077-1088, 10 2017.
- [5] E. Fawcett, "Spin-density-wave antiferromagnetism in chromium," *Reviews of Modern Physics*, vol. 60, pp. 209-283, 1 1988.
- [6] T. Onozaki, Y. Toda, S. Tanda and R. Morita, "Coherent Double-Pulse Excitation of Charge-Density-Wave Oscillation," *Japanese Journal of Applied Physics*, vol. 46, pp. 870-872, 2 2007.
- [7] M. Chollet, R. Alonso-Mori, M. Cammarata, D. Damiani, J. Defever, J. T. Delor, Y. Feng, J. M. Glowia, J. B. Langton, S. Nelson, K. Ramsey, A. Robert, M. Sikorski, S. Song, D. Stefanescu, V. Srinivasan, D. Zhu, H. T. Lemke and D. M. Fritz, "The X-ray Pump--Probe instrument at the Linac Coherent Light Source," *Journal of Synchrotron Radiation*, vol. 22, pp. 503-507, 2015.
- [8] A. Singer, S. Patel, R. Kukreja, V. Uhlíř, J. Wingert, S. Festersen, D. Zhu, J. Glowia, H. Lemke, S. Nelson, M. Kozina, K. Rossnagel, M. Bauer, B. Murphy, O. Magnussen, E.

- Fullerton and O. Shpyrko, "Photoinduced Enhancement of the Charge Density Wave Amplitude," *Physical Review Letters*, vol. 117, 7 2016.
- [9] K. W. Kim, A. Pashkin, H. Schäfer, M. Beyer, M. Porer, T. Wolf, C. Bernhard, J. Demsar, R. Huber and A. Leitenstorfer, "Ultrafast transient generation of spin-density-wave order in the normal state of BaFe₂As₂ driven by coherent lattice vibrations," *Nature Materials*, vol. 11, pp. 497-501, 4 2012.
- [10] E. Torrontegui, S. Ibáñez, S. Martínez-Garaot, M. Modugno, A. del Campo, D. Guéry-Odelin, A. Ruschhaupt, X. Chen and J. G. Muga, "Shortcuts to Adiabaticity," in *Advances In Atomic, Molecular, and Optical Physics*, Elsevier, 2013, pp. 117-169.
- [11] S. Deffner, C. Jarzynski and A. del Campo, "Classical and Quantum Shortcuts to Adiabaticity for Scale-Invariant Driving," *Physical Review X*, vol. 4, 4 2014.
- [12] B. B. Zhou, A. Baksic, H. Ribeiro, C. G. Yale, F. J. Heremans, P. C. Jerger, A. Auer, G. Burkard, A. A. Clerk and D. D. Awschalom, "Accelerated quantum control using superadiabatic dynamics in a solid-state lambda system," *Nature Physics*, vol. 13, pp. 330-334, 11 2016.
- [13] I. Vaskivskiy, I. A. Mihailovic, S. Brazovskii, J. Gospodaric, T. Mertelj, D. Svetin, P. Sutar and D. Mihailovic, "Fast electronic resistance switching involving hidden charge density wave states," *Nature Communications*, vol. 7, 5 2016.
- [14] A. Zong, X. Shen, A. Kogar, L. Ye, C. Marks, D. Chowdhury, T. Rohwer, B. Freelon, S. Weathersby, R. Li, J. Yang, J. Checkelsky, X. Wang and N. Gedik, "Ultrafast manipulation of mirror domain walls in a charge density wave," *Science Advances*, vol. 4, p. eaau5501, 10 2018.
- [15] V. Baltz, A. Manchon, M. Tsoi, T. Moriyama, T. Ono and Y. Tserkovnyak, "Antiferromagnetic spintronics," *Reviews of Modern Physics*, vol. 90, 2 2018.
- [16] P. Němec, M. Fiebig, T. Kampfrath and A. V. Kimel, "Antiferromagnetic opto-spintronics," *Nature Physics*, vol. 14, pp. 229-241, 3 2018.
- [17] A. M. N. Niklasson, B. Johansson and L. Nordström, "Spin Density Waves in Thin Chromium Films," *Physical Review Letters*, vol. 82, pp. 4544-4547, 5 1999.
- [18] A. Singer, S. K. K. Patel, V. Uhlíř, R. Kukreja, A. Ulvestad, E. M. Dufresne, A. R. Sandy, E. E. Fullerton and O. G. Shpyrko, "Phase coexistence and pinning of charge density waves by interfaces in chromium," *Physical Review B*, vol. 94, 11 2016.
- [19] M. Fechner, A. Sukhov, L. Chotorlishvili, C. Kenel, J. Berakdar and N. A. Spaldin, "Magnetophononics: Ultrafast spin control through the lattice," *Physical Review Materials*, vol. 2, 6 2018.
- [20] A. Subedi, A. Cavalleri and A. Georges, "Theory of nonlinear phononics for coherent light control of solids," *Physical Review B*, vol. 89, 6 2014.
- [21] A. Singer, M. J. Marsh, S. H. Dietze, V. Uhlíř, Y. Li, D. A. Walko, E. M. Dufresne, G. Srajer, M. P. Cosgriff, P. G. Evans, E. E. Fullerton and O. G. Shpyrko, "Condensation of collective charge ordering in chromium," *Physical Review B*, vol. 91, 3 2015.
- [22] J. P. Hill, G. Helgesen and D. Gibbs, "X-ray-scattering study of charge- and spin-density waves in chromium," *Physical Review B*, vol. 51, pp. 10336-10344, 4 1995.

- [23] V. R. Morrison, R. P. Chatelain, K. L. Tiwari, A. Hendaoui, A. Bruhács, M. Chaker and B. J. Siwick, "A photoinduced metal-like phase of monoclinic VO₂ revealed by ultrafast electron diffraction," *Science*, vol. 346, pp. 445-448, 10 2014.
- [24] A. Kogar, A. Zong, P. E. Dolgirev, X. Shen, J. Straquadine, Y.-Q. Bie, X. Wang, T. Rohwer, I.-C. Tung, Y. Yang, R. Li, J. Yang, S. Weathersby, S. Park, M. E. Kozina, E. J. Sie, H. Wen, P. Jarillo-Herrero, I. R. Fisher, X. Wang and N. Gedik, "Light-induced charge density wave in LaTe₃," *Nature Physics*, 11 2019.
- [25] R. Yusupov, T. Mertelj, V. V. Kabanov, S. Brazovskii, P. Kusar, J.-H. Chu, I. R. Fisher and D. Mihailovic, "Coherent dynamics of macroscopic electronic order through a symmetry breaking transition," *Nature Physics*, vol. 6, pp. 681-684, 8 2010.
- [26] S. D. Brorson, A. Kazeroonian, J. S. Moodera, D. W. Face, T. K. Cheng, E. P. Ippen, M. S. Dresselhaus and G. Dresselhaus, "Femtosecond room-temperature measurement of the electron-phonon coupling constant in metallic superconductors," *Physical Review Letters*, vol. 64, pp. 2172-2175, 4 1990.
- [27] C. Nicholson, C. Monney, R. Carley, B. Frietsch, J. Bowlan, M. Weinelt and M. Wolf, "Ultrafast Spin Density Wave Transition in Chromium Governed by Thermalized Electron Gas," *Physical Review Letters*, vol. 117, 9 2016.
- [28] L. M. Corliss, J. M. Hastings and R. J. Weiss, "Antiphase Antiferromagnetic Structure of Chromium," *Physical Review Letters*, vol. 3, pp. 211-212, 9 1959.
- [29] H. J. Zeiger, J. Vidal, T. K. Cheng, E. P. Ippen, G. Dresselhaus and M. S. Dresselhaus, "Theory for displacive excitation of coherent phonons," *Physical Review B*, vol. 45, pp. 768-778, 1 1992.
- [30] L. D. Landau and E. M. Lifshitz, *Statistical Physics*, Elsevier Science & Technology, 1996.

Figures

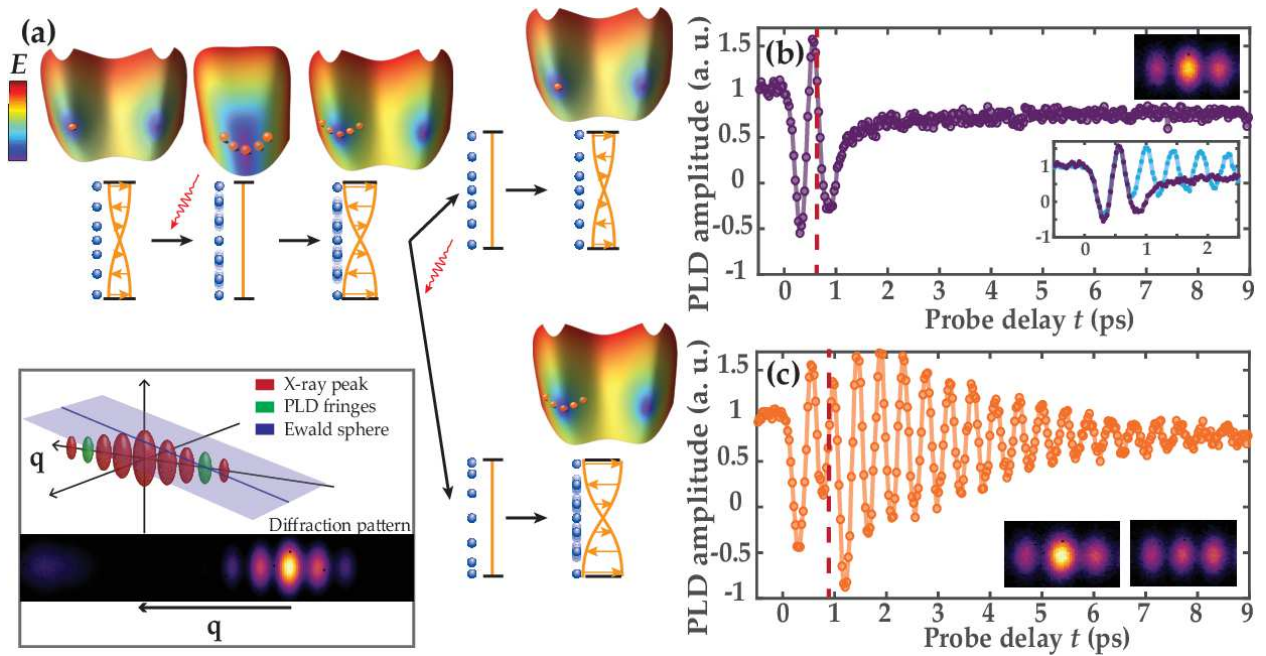


Fig. 1. Controlled enhancement and destruction of the excited state. **a**, A laser pulse excites the system by destroying the magnetic order; a second pulse either excites the released phonon further or stops the excitation. Schematic energy surfaces show the PLD state as the orange point. Inset: x-ray scattering from periodic atomic displacement is detected on a fringe of the main peak from the crystalline film. **b**, **c**, Amplitude of the PLD in two extreme control cases. Solid lines are experimental data (empty circles) - connected. The dashed red line marks the time of second pulse arrival. **b** - $(\tau_2 - \tau_1)$ delay of 620 fs. Top inset shows the Laue fringe with the satellite peak after the suppression of the excited state. Bottom inset compares PLD amplitude with single pulse (blue) to two pulses (purple). **c** - $(\tau_2 - \tau_1)$ delay of 845 fs. Inset shows the Laue fringe with the satellite peak at maximum and minimum PLD values.

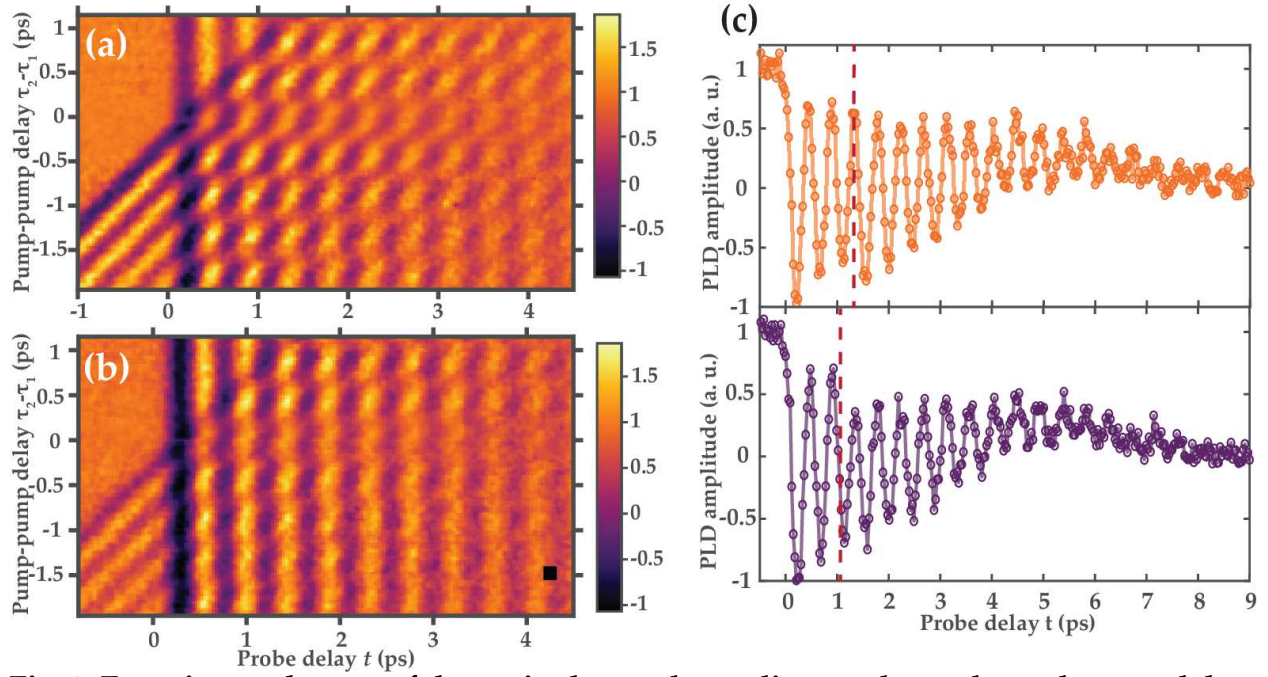


Fig. 2. Experimental maps of the excited state depending on the probe and pump delay. **a**, Map of the PLD amplitude before and after excitation by two pulses with a fluence of 1.45 mJ/cm^2 . **b**, Map of the PLD amplitude before and after excitation by two pulses with the second pulse intensity weakened by a factor of 2. **c**, Magnitude of the PLD in “enhancement” and “suppression” conditions at laser pulse fluence 9.5 mJ/cm^2 for the first pulse and 4.7 mJ/cm^2 for the second pulse. Solid lines are experimental data (empty circles) connected. The dashed red line marks the time of second pulse arrival. **top** $-\tau_2 - \tau_1$ of 1295 fs, **bottom** $-\tau_2 - \tau_1$ of 1065 fs.

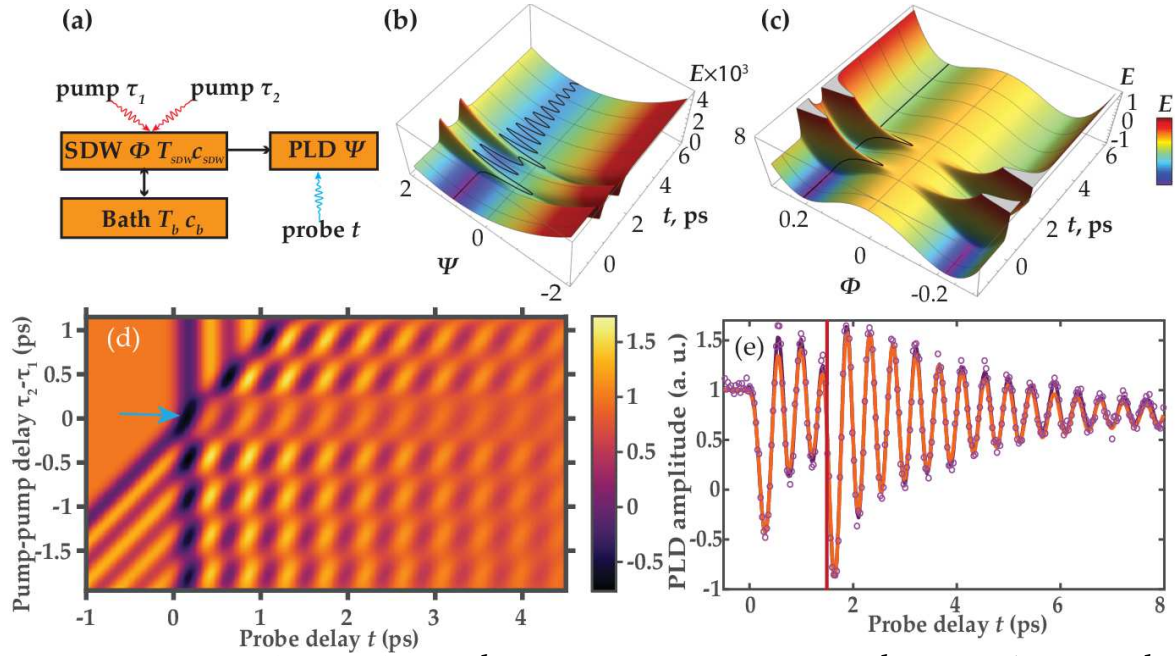


Fig. 3. Theoretical model. **a**, Schematic representation of the model. **b**, **c** Schematic evolutions of y and L on their respective potential surfaces. The color accentuates the surface shape for illustration purposes. **d**, Color map of the simulated amplitude of the acoustic mode, depending on pump-pump, and pump-probe delay. The faint row, highlighted by the blue arrow, at 0 ps pump-pump delay demonstrates the weaker excitation by a single high-fluence pulse. Higher amplitudes are achieved at higher pump-pump delay times. **e**, Typical example of the fit achieved by the model. Purple line is the experimental data (empty circles) smoothed by a Savitzky-Golay filter, orange line is the theoretical model. The red line marks the time of second pulse arrival.

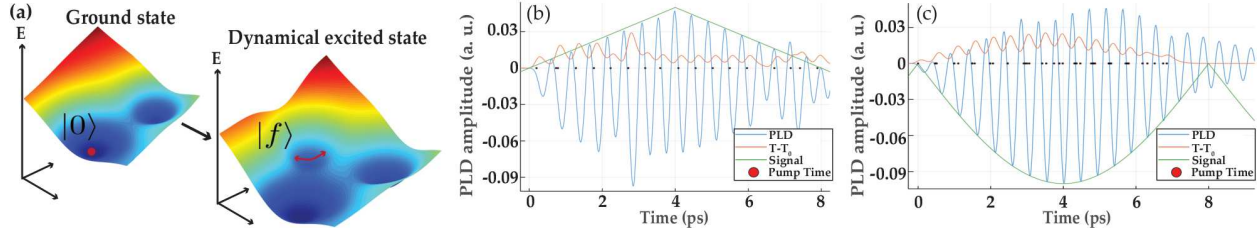


Fig. 4. Simulation of a pulse train excitation. **a**, Phenomenology for advanced control, suspending the system in an excited state. **b**, **c**, Optimal control of the oscillation, guiding the envelope of the signal along the desired **(b)** triangular or **(c)** sinusoidal curve (in green) by applying a train of pulses with the same fluence, timed at the moments indicated by purple circles on the horizontal axis. The deviation from the initial temperature is plotted in orange. The simulations used the model parameters determined from the experiment.

Methods

A. Film preparation

The thin chromium film was deposited onto the single-crystal MgO(001) substrate using DC magnetron sputtering at a substrate temperature of 500° C and annealed for 1 h at 800° C. The growth process was optimized to yield both a smooth surface and good crystal quality of the sample. The film thickness was determined to be 28 nm by x-ray diffraction. The Néel temperature of a thin film is reduced to 290 K.

B. Experimental parameters

The pump-probe experiment was carried out at the XPP instrument of the LCLS with an x-ray photon energy of 8.9 keV, selected by the (111) diffraction of a diamond crystal. X-ray diffraction in the vicinity of the out of plane (002) Bragg peak ($2\theta=60$ degrees) from each pulse was recorded by an area detector (CS140k) with a repetition rate of 120 Hz. Due to the mosaic spread of the crystal in the film plane, a number of Laue oscillations are observed on the area detector simultaneously. About 100 pulses were recorded for each time delay (50 fs steps in the time traces). For each time delay, the intensity was dark noise corrected and normalized by the intensity measured in the region of the area detector where Laue oscillations were absent. The sample was excited by optical (800 nm, 40-fs), p-polarized laser pulses propagating nearly collinear with the x-ray pulses. The final temporal resolution was estimated to be 80 fs. The spot sizes (full width at half maximum) of the optical and x-ray pulses were 0.46 mm (H) \times 0.56 mm (V) and 0.2 mm (H) \times 0.2 mm (V), respectively. The combined power of both optical laser pulses in measurements without filters was 2.9 mJ/cm² in standard runs and 19 mJ/cm² in high power runs. A 0.3 OD ND filter with a transmittance of 0.5 was used to weaken the second laser pulse in the relevant measurements.

C. Theoretical fit parameters

The fit is performed using equations of motion derived from the Lagrangian of the system

$$L = \frac{m_\Phi(\dot{L} + \gamma_L L)^2}{2} + \frac{m_\Psi(\dot{\Psi} + \gamma_\Psi \Psi)^2}{2} - F,$$

$$m_\Phi \ddot{\Phi} = -\alpha(T_{SDW} - T_N)L - \beta L^3 + 2gL\Psi - \gamma_\Phi \dot{L},$$

$$m_\Psi \ddot{\Psi} = gL^2 - \omega_0^2 \Psi - b\Psi^3 - \gamma_\Psi \dot{\Psi},$$

where γ_L and γ_Ψ are damping parameters, and the two-temperature model is described in the text. Gray box fitting of the differential equations was performed using the output PDL amplitude Ψ and known parameters, that is pulse arrival time and critical temperature. To describe the heat injection from the photon pulses, and subsequent transfer between spin degrees of freedom (T_{SDW}) and a thermal bath (T_b , all non-primary phonons), we use a two-temperature model,

$$c_{SDW} T'_{SDW} = -k[T_{SDW}(t) - T_b(t)] + Q_{ph}(t), \quad (2)$$

$$c_b T'_b = -k[T_b(t) - T_{SDW}(t)] \quad (3)$$

where $Q_{ph}(t) \sim Ae^{-(t-t_0)^2/\tau^2}$ is the heat injected by the photon pulses and primes designate time derivative. The parameters in the model defined in eq (1-3) extracted from the fit are $\alpha = 6039$, $\beta = 7.97$, $g = 0.52$, $\omega_0 = 14.11$, $b = 3.38e8$, $c_L = 0.36$, $c_b = 3.58$, $k = 1.29$.

D. Verification of experimental observations

We have verified that we do not observe a timescale associated with removal of topological defects. First, removal of topological defects would lead to a decrease of the disorder in the domain structure, causing an increase in the width of the scattering from

the PLD and a corresponding decrease of the satellite X-ray peak intensity, which is not observed. Second, while the change in pulse intensity does cause a slight increase in the order recovery time [8], the increase is not as significant as in [3] [31] [32], and can instead be explained sufficiently by temperature difference [8, 27]. The absence of topological timescale in our data can be explained by a low film thickness that inhibits all but one SDW wavevector direction, causing the domains to not form in the “depth” of the film. Additionally, it suggests that the domain boundaries splitting the film surface are enforced extrinsically by defects in the structure.

Additional Bibliography (Methods)

[31] A. Zong, P. E. Dolgirev, A. Kogar, E. Ergeçen, M. B. Yilmaz, Y.-Q. Bie, T. Rohwer, I.-C. Tung, J. Straquadine, X. Wang, Y. Yang, X. Shen, R. Li, J. Yang, S. Park, M. C. Hoffmann, B. K. Ofori-Okai, M. E. Kozina, H. Wen, X. Wang, I. R. Fisher, P. Jarillo-Herrero and N. Gedik, "Dynamical Slowing-Down in an Ultrafast Photoinduced Phase Transition," *Physical Review Letters*, vol. 123, 8 2019.

[32] P. E. Dolgirev, M. H. Michael, A. Zong, N. Gedik and E. Demler, "Universal dynamics of order parameter fluctuations in pump-probe experiments," 6 10 2019.

Figures

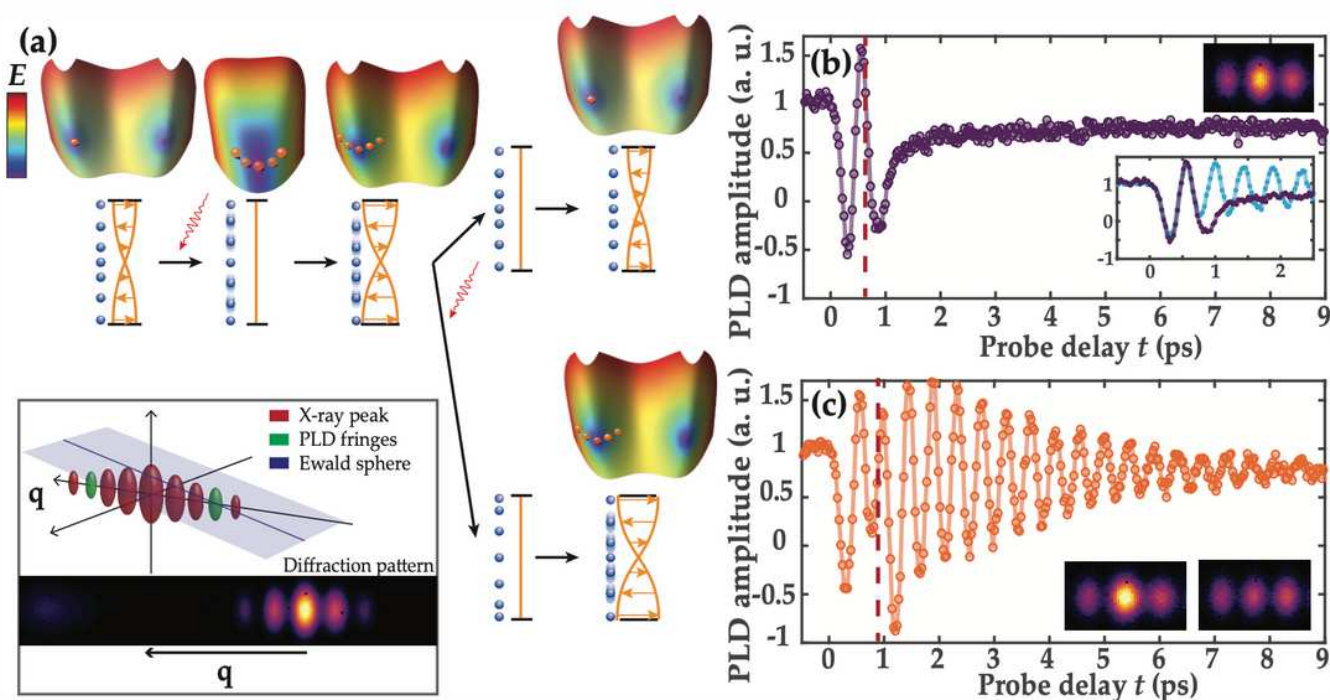


Figure 1

Controlled enhancement and destruction of the excited state. a, A laser pulse excites the system by destroying the magnetic order; a second pulse either excites the released phonon further or stops the excitation. Schematic energy surfaces show the PLD state as the orange point. Inset: x-ray scattering from periodic atomic displacement is detected on a fringe of the main peak from the crystalline film. b, c, Amplitude of the PLD in two extreme control cases. Solid lines are experimental data (empty circles) - connected. The dashed red line marks the time of second pulse arrival. b – $(\tau_2 - \tau_1)$ delay of 620 fs. Top inset shows the Laue fringe with the satellite peak after the suppression of the excited state. Bottom inset compares PLD amplitude with single pulse (blue) to two pulses (purple). c – $(\tau_2 - \tau_1)$ delay of 845 fs. Insets show the Laue fringe with the satellite peak at maximum and minimum PLD values.

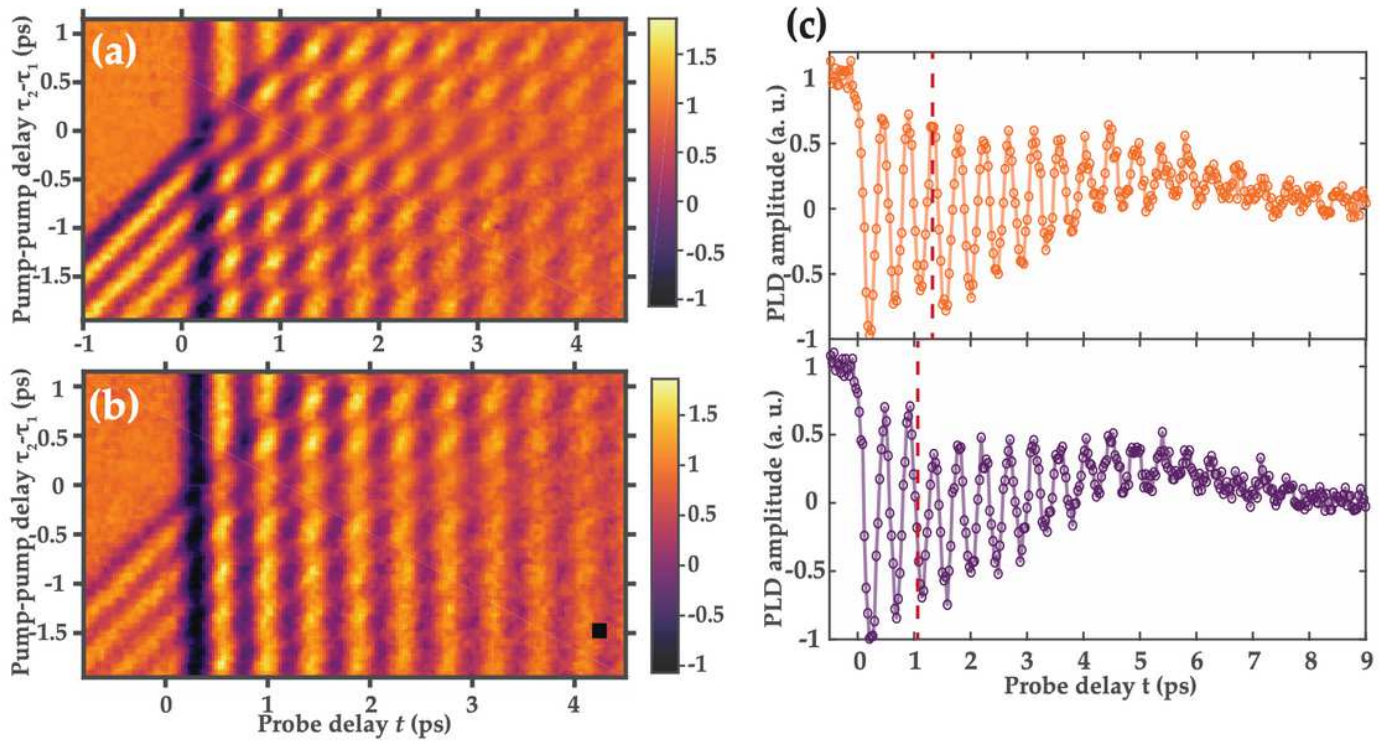


Figure 2

Experimental maps of the excited state depending on the probe and pump delay. a, Map of the PLD amplitude before and after excitation by two pulses with a fluence of 1.45 mJ/cm². b, Map of the PLD amplitude before and after excitation by two pulses with the second pulse intensity weakened by a factor of 2. c, Magnitude of the PLD in “enhancement” and “suppression” conditions at laser pulse fluence 9.5 mJ/cm² for the first pulse and 4.7 mJ/cm² for the second pulse. Solid lines are experimental data (empty circles) connected. The dashed red line marks the time of second pulse arrival. top – $\tau_2 - \tau_1$ of 1295 fs, bottom – $\tau_2 - \tau_1$ of 1065 fs.

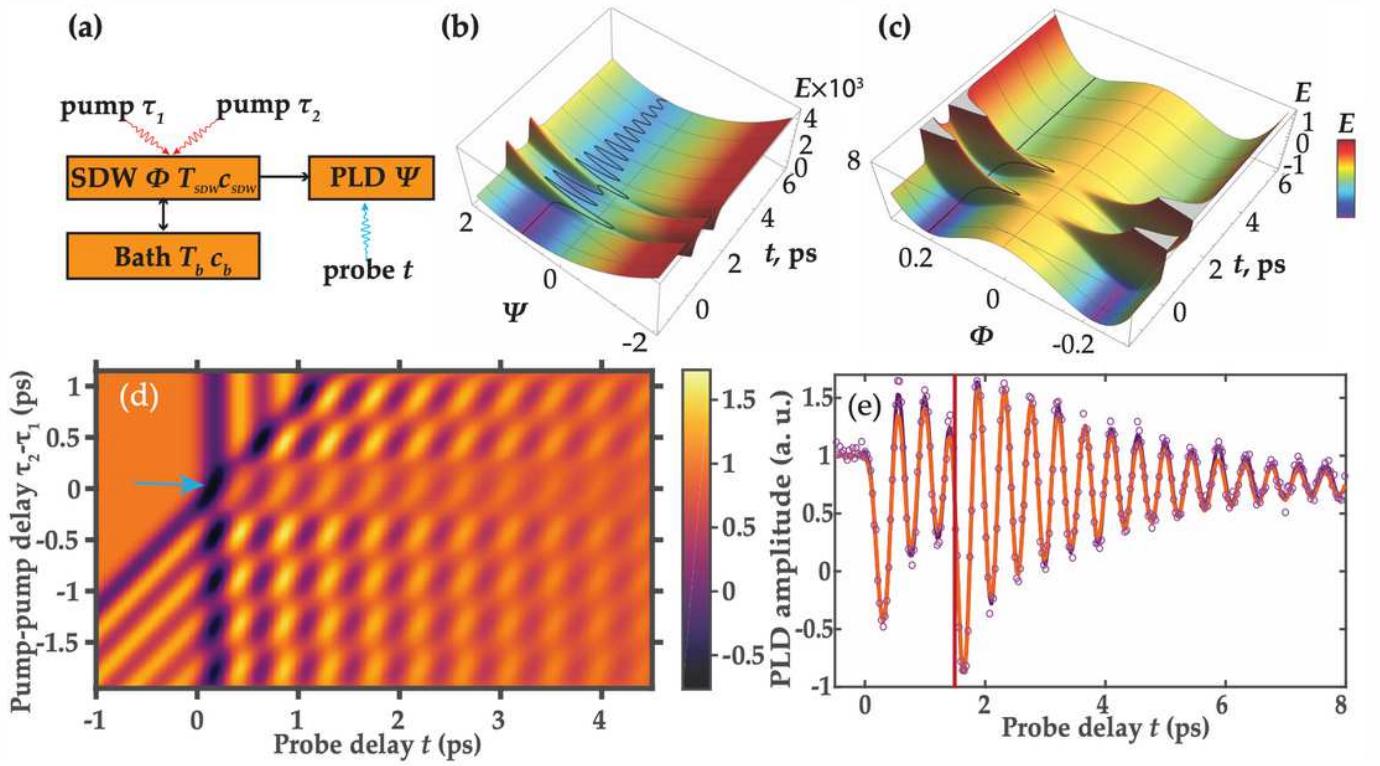


Figure 3

Theoretical model. a, Schematic representation of the model. b, c Schematic evolutions of y and L on their respective potential surfaces. The color accentuates the surface shape for illustration purposes. d, Color map of the simulated amplitude of the acoustic mode, depending on pump-pump, and pump-probe delay. The faint row, highlighted by the blue arrow, at 0 ps pump-pump delay demonstrates the weaker excitation by a single high-fluence pulse. Higher amplitudes are achieved at higher pump-pump delay times. e, Typical example of the fit achieved by the model. Purple line is the experimental data (empty circles) smoothed by a Savitzky-Golay filter, orange line is the theoretical model. The red line marks the time of second pulse arrival.

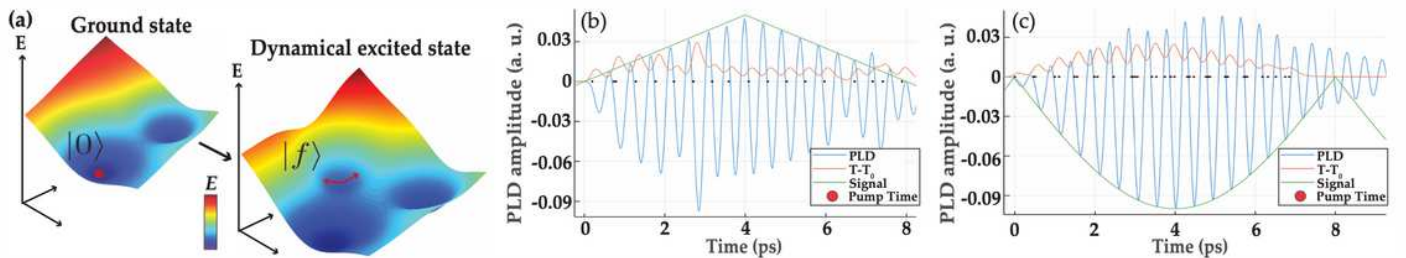


Figure 4

Simulation of a pulse train excitation. a, Phenomenology for advanced control, suspending the system in an excited state. b, c, Optimal control of the oscillation, guiding the envelope of the signal along the

desired (b) triangular or (c) sinusoidal curve (in green) by applying a train of pulses with the same fluence, timed at the moments indicated by purple circles on the horizontal axis. The deviation from the initial temperature is plotted in orange. The simulations used the model parameters determined from the experiment.